IMPROVED DESIGN OF SINGLE-LAYERED WIRE STRAND FOR COMBINED TENSILE AND CRIMPING TESTING WITH MESH ELEMENT OPTIMIZATION

Guillaume Cadet, Manuel Paredes, Herve Orciere

IMPROVED DESIGN OF SINGLE-LAYERED WIRE STRAND FOR COMBINED TENSILE AND CRIMPING TESTING WITH MESH ELEMENT OPTIMIZATION

Authors
Guillaume Cadet, ICA, Université de Toulouse, UPS, INSA, ISAE-SUPAERO, MINES-ALBI, CNRS, 3 rue Caroline Aigle, 31400 Toulouse, France, +33 6 99 10 92 22, cadet@insa-toulouse.fr
Manuel Paredes, ICA, Université de Toulouse, UPS, INSA, ISAE-SUPAERO, MINES-ALBI, CNRS, 3 rue Caroline Aigle, 31400 Toulouse, France, +33 6 21 58 66 56, paredes@insa-toulouse.fr
Hervé Orcière, CGR International, Avenue Jean Moulin, Zone activité du plat, 05400 Veynes, France, +33 6 33 94 02 81, herve.orciere@cgr-international.com

Corresponding author
Manuel Paredes: paredes@insa-toulouse.fr

Dyna ; Volume 98 Issue 3 Page 274-281 DOI 10.6036/10677

ABSTRACT:
Faced with increasing competition in the global automotive market, reducing costs and design time has become a major focus of development among manufacturers. Faced with these needs, the numerical simulation of shaping processes has become an essential tool. It saves considerable time in the upstream phase of a project by reducing the number of experimental campaigns on prototypes. The studied mechanical system consists mainly in a part crimping at one end of a multi-stranded wire rope, which is stressed in tension. In order to reduce calculation time, it is important to get the optimal meshing parameters which provide a high accuracy. In this paper, a numerical model of a single layered wire rope is studied. The objective is to determine the optimal size and shape of meshing elements to get both accurate and fast results. First of all, the wire strand is investigated in tension and compared with the analytical formulation by G.Costello. Then, the organized wire strand is investigated in crimping process for the first time. The process reveals the optimal solution is with 16 elements in the diameter of the wire and 15 times longer than wider. This model is then used to simulate the behavior of a strand in a first-ever combined crimping-tensile test in order to obtain a minimal crimping length. This work can be very important for designers to reduce considerably the calculation time of their numerical models while guarantying a great accuracy in the mechanical behavior of a wire rope.

Keywords: Wire rope, Finite element simulation, meshing process, optimization, Mesh elements parameters optimization, Single-layered wire strand numerical model, Wire strand optimal mesh parameters, Wire rope crimping simulation, Tensile stressed wire strand

FUNDING
This research did not receive any specific grant from funding agencies in the public, commercial, or not-for-profit sectors.

NOTATION:

D	mm	Diameter of a wire
E	MPa	Young's modulus
e_D	-	Number of elements along the diameter of the wire
e_L	-	Number of elements along the length of the wire
F	N	Axial force
k	-	Ratio of the length over the width of an element
L	mm	Length of the strand
r_1	mm	Radius of the central core
r_2	mm	Radius of the external wires
r_s	mm	Wound radius of the external wires
N_s	-	Number of external wires in the strand
x_s, y_s, z_s	mm	Coordinates of the mean curve of a helical wire
α_s	°	Lay angle of the external wires

ξ_1	-	Axial strain of the central core
ξ_2	-	Axial strain of the external wires
θ_s	°	Coordinate of wounding of the mean curve of a helical wire
θ_{Ns}	°	Angle of phase difference between external wires
ν	-	Poisson's ratio
τ_s	°	Torsion angle of the ends of the wires
κ'_s	mm^{-1}	Curvature of the external wires

1 - INTRODUCTION

Faced with increasing competition in the global automotive market, reducing costs and design time has become a major focus of development among manufacturers. The desire to reduce the weight of the vehicle has become not only an important competitive issue, but also an environmental constraint. Faced with these needs, the numerical simulation of shaping processes has become an essential tool. It saves considerable time in the upstream phase of a project to ensure the feasibility of parts or the development of a new innovative shaping process. Indeed, the objective of the simulation is to reduce the number of experimental campaigns on prototypes or test samples, considered too long and too expensive. Over the past ten years, finite element simulations have evolved considerably in the field of metal part forming.

The studied mechanical system consists mainly in a part crimping an end of a wire rope, which is stressed in tension. The task is the modelling of the crimping process of the cable and then the mechanical analysis of the structure under several stresses. The studied wire rope is made from one straight and six simple helical wires in contact with each other. In order to reduce the calculation time, it is important to get the optimal meshing parameters which always guarantee a high accuracy.

2 – LITTERATURE REVIEW

Helical geometries like wire ropes are found in many applications such as mechanical engineering [1,2], civil engineering [1], electrical engineering [2] or biological engineering [3]. A helical shape can be created either by molding or by deformation of a straight material.

Helical mechanical behavior began to be treated in 1892 by A.E.H. Love in his book 'A Treatise on the Mathematical Theory of Elasticity' [4]. However, the mechanical behaviors of cables are more investigated in the work of S. Timoshenko [5]. In this reference book published in 1930, a chapter is devoted to springs having a constant pitch, thus representing the exact geometry of an undeformed helix. Pioneer studies focused on the behavior of multi-stranded cables were published some years later by F. Hruska, A.E. Green and N. Laws, and E. Kroner [6,7,8].

The theory of A.E.H. Love [4] was taken up by A. Costello [9] in order to apply it to curved bars and multi-strand cables. Its equilibrium equations are used to understand the mechanical behavior of various cables (straight and simple helical strands, Independent Wire Rope Core - IWRC - and Seale formations). As an example, he formulated the equation of the axial load F (1). This load depends on the elongation (central core axial strain ξ_1, strand's wires axial strain ξ_2 and curvature κ'_s) but also on the angle of torsion of the ends (τ_s). The radii r_1, r_2 and r_s are respectively the radius of the central core, the radius of the helical wires and the wound radius of the helical wires.

$$F = \pi\xi_1 E r_1^2 + N_s E r_2^2 \left(\pi\xi_2 \sin(\alpha_s) + \frac{\left(\frac{\pi r_2 \Delta\kappa' s}{4}\sin(\alpha_s) + \frac{\pi r_2 \Delta\tau_s}{4(1+\nu)}\cos(\alpha_s)\right) r_2}{r_s}\cos^2(\alpha_s) \right) \qquad (1)$$

This equation makes it possible to quickly obtain the elastic behavior of a cable or strand. However, no studies have been conducted on the analytical or numerical analysis of the pressure forces that a strand or cable would undergo by radial compression, as it could undergo during a crimping.

In the early 70s, finite element methods were applied to cable analysis. W. Zhou and H.Q. Tian [10] propose a design of a strand by polar coordinates within a Cartesian coordinate system. Thus, the design of the geometry of their finite element model is very complex. They decide to load their model in flexion and then tension. The results obtained correlate well with Costello's theory.

More recently, Wang et al [11] have investigated the coupling effect of tension and reverse torque during axial tension of a wire strand. Other studies, dealing with a simple strand [12-13] have recreated a finite element model that considers the advantage of helical symmetry. Based on Costello's theory, they find more precise results in the calculation of the response of the strand to the axial forces of tension and torsion. This type of model also highlights the non-linear effects related to contact stresses, residual stresses [14], friction and plastic deformation which are very difficult phenomena to reveal analytically but which play an important role in the rupture of cables.

I. Gerdemeli [15] and Y.J. Chiang [16] conducted a fatigue life study of a single strand. The helical wires are created by sweeping with a non-orthogonal section. They therefore obtain a very simple profile guide curve (a straight line) but get a much more complex formulation of the geometry of the section. Moreover, this can induce a problem for a lower helix angle as the hypothesis is then no longer valid [17].

The study conducted by C. Erdönmez [18] is unique in the creation of an average line of the non-straight cable. Indeed, the tests are carried out by modelling a single strand wound around a pulley. Unfortunately, it does not give any mathematical model justifying it so that it can be reproduced.

But most studies [1, 19-21] build their single-helix wires by sweeping a circular cross-section normal to the guide curve. This is the simplest method to implement on most finite element software. Indeed, in a minimum of parameters, we obtain the volumes of the different wires.

Mesh allows the geometry of parts to be discretized into smaller pieces called elements. The choice of the type of elements is crucial to try to predict the behavior of the material as accurately as possible [22, 23] while minimizing the calculation time. 3D finite element software commonly exploits four different forms of three-dimensional elements: bricks, prismatic, pyramidal and tetrahedral. Triangular shapes cause the unwanted increase of the elements' stiffness and therefore of the solid. Here, only the brick avoids this problem by proposing an element with six square faces. Most of the time, designers use cubic shapes to design their elements (each edge is equally sized) as in [24]. But in order to reduce the calculation time, it is possible to make the element longer than wider without losing in accuracy. It depends on the direction of the solicitations and the element type. J.Cho [25] mixed solid and truss elements to obtain more accurate results for a cord with combined stresses.

In [26], the authors make comparisons of the mechanical performance of a metal vascular stent (tubular) and bioresorbable polymers during a crimping phase. In particular, they study the effects of residual crimping stresses on stent expansion. For this, they choose brick elements with incompatible mode [27] to avoid shear locking which helps stiffening the underloaded structure in bending.

Other studies [28-31], brick elements with reduced integration. The reduced integration process is only applicable to quadrilateral and hexahedral elements (bricks) [27]. With this process, linear elements with 8 integration nodes have only one, positioned at the centroid of the element. Quadratic elements go from 20 to 8 integration points. Thus, the calculation time is greatly reduced. Linear elements with reduced integration are very tolerant to distortion. Therefore, using a fine mesh of these elements in any simulation where distortion levels can be very high is necessary. Linear elements with reduced integration therefore tend to be too flexible because they suffer from their own digital problem 'Hourglass' [32]. In Abaqus software, a small amount of artificial 'Hourglass' stiffness is introduced into the first-order reduced integration elements to limit the spread of hourglass modes.

Crimping is a process with great deformation involving a significant bending of the initial elements. It also requires the use of relatively small mesh sizes in order to correctly reproduce the high deformation. One solution is to use a very thin mesh from the beginning and uniform throughout the part, at the cost of high calculation time. The interest of mesh refinement is to refine the highly constrained or contact areas to the detriment of other less solicited regions and to save precious time for a comparable or even better results accuracy. The mesh refinement procedure can be performed during the design phase [33] or can be adaptive [32, 34, 35].

The size of the different elements is also an important step when creating the model. This is, along with the number and duration of iterations, the most decisive factor on the calculation time. It is therefore essential to optimize your decision-making and make a compromise between [32]:

- Decrease the size of the elements in the crimping phase to increase the accuracy of the calculations
- Reduce their size to avoid stiffening the structure
- Increase their size to reduce the number of nodes, therefore the number of unknowns and reduce the calculation time.

The first goal of this study is to define the meshing parameters in a case of a 7 wires strand, independently tested in crimping and tension. The targets are the accuracy of the model and the calculation time. Then, the second goal is to simulate the strand in combined tension and crimping to minimize the crimping length without modifying the strength of the assembly.

3 – NUMERICAL STUDY
3.1 – INVESTIGATED STRAND

The tested wire rope is a single layer strand, right lay, composed of one central straight core and 6 wires wound around it. Its geometric properties are detailed in Table 1.

Diameter of the central wire core	d_1	0.59 mm
Diameter of the external wires	d_2	0.53 mm
Youngs' modulus	E	175,000MPa
Poison's ratio	v	0.29
Lay angle	α	80°

Table 1. Wire strand geometric property

Thus, using the studies mentioned above, we define the following single helix wire's mean curve equations by creating a spline linking a predefined number of increment points, corresponding to the centroidal line of the external wires:

$$x_s = r_s \cos(\theta_s + \theta_{Ns}) \quad (2)$$

$$y_s = r_s \sin(\theta_s + \theta_{Ns}) \quad (3)$$

$$z_s = r_s \tan(\alpha_s)\theta_s \quad (4)$$

With:

$$\theta_{Ns} = \frac{2\pi}{N_s} \quad (5)$$

$$\theta_s = \frac{L}{r_s \tan(\alpha_s)} \quad (6)$$

The first helical wire is generated by sweeping a circular cross section along the helix defined above. The five other helical wires are created by circular repetition. To ensure that the wires do not penetrate each other at the initial state, a small geometrical gap is introduced.

Both models only consider the elastic behavior of the material. Every contact between each part are managed individually. The tensile test is frictionless to fit with Costello's analytical formulation. The crimping test uses a friction coefficient of 0.35.

For the tensile testing, the model, visible in Fig. 1.a, is 40mm long. Both ends are coupled (i.e. all the seven wires end can't move in relation to each other). One extremity is fixed and the other is constrained with an axial constant velocity (every other degrees of freedom are fixed).

For the crimping testing, the model, visible in Fig. 1.b, is 20mm long. Six rigid semi-cylindrical tiles of length 15mm are placed around the strand to simulate the crimping process and to avoid non-symmetrical behavior. The crimping depth is set to 0.07mm. One extremity is coupled with a reference point that is fixed, 5mm away of the tiles to observe the edges effects. The other end is free. For the first time, an organized wire strand is studied in a radially stressed 3D simulation.

Fig. 1. Models of tensile test (a) and crimping test (b)

3.2 – MESH PROPERTIES

In In addition to the complex geometry of a strand, it is also difficult to properly mesh such parts. Indeed, a profile with a circular section leads to two mesh difficulties. The first is the verification of the homogeneity of the shape of the elements near the central point [36] (Figure 2). The second is the verification of the good fluidity of the elements along the curvatures of the average line. To ensure a good mesh shape quality [37], we split the cross section in four parts and affect seeds along the edges.

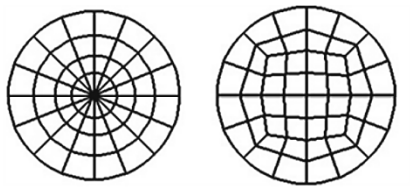

Fig. 2. Circular cross-section meshing quality: low (left), high (right)

According to the previous studies, we choose bricks elements with reduced integration with an Implicit Dynamic solving. In that way, we avoid triangular elements in 2D or 3D which can stiffen the whole part.

With D the diameter of the wire, L its length, e_D the number of elements in the diameter and e_L the number of elements over the length. Let k, the ratio of the length over the width of the element, be:

$$k = \frac{L\, e_D}{D\, e_L} \tag{7}$$

Then, the two non-dimensional parameters we can use as variables are the number of the element by diameter e_D and the ratio k. This is important to carry a general solution of the mesh designing parameters. The cross-section mesh resolution covers number of elements in the diameter from 4 (low resolution) to 20 (high resolution) as seen in Fig. 3. The axial mesh resolution covers length over width ratio from 2 (high resolution) to 20 (low resolution) as seen in Fig. 4.

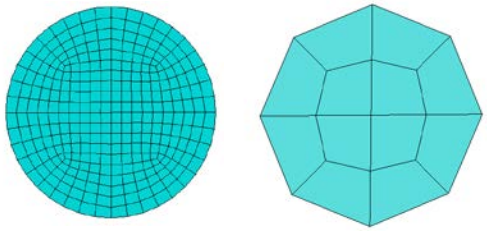

Fig. 3. Cross section meshing with e_D =20 (left) and e_D =4 (right)

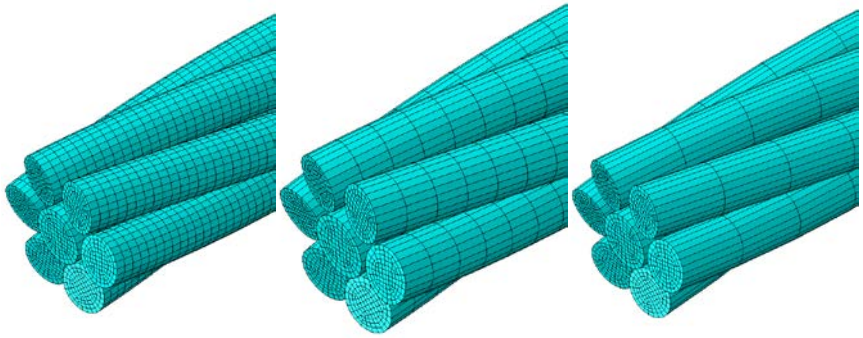

Fig. 4. Axial meshing with k =2 (left), k =6 (middle) and k =15 (right)

4 – RESULTS AND DISCUSSION

4.1 – TENSILE TEST

The two target outputs are the calculation time and the stiffness error. This error evaluation is made in comparison to the analytical one, from Equation (1) made by G.A. Costello. For fixed ends, we obtain a global stiffness of 2690N/mm. The sampling process is made to represent the most accurately the range of designing parameters with a numerical campaign time reasonably short.

Error (%)		e_D								
		20	18	16	14	12	10	8	6	4
k	2			-2.61		-3.55		-7.16	-11.04	
	3	-2.67			-3.21		-4.60		-11.10	
	4		-2.30			-3.54		-5.80		-34.10
	5			-2.93			-5.07		-9.40	
	6				-3.14	-3.54		-6.40	-12.20	
	8						-5.08			
	10	-2.36				-3.83		-6.26	-12.59	
	12		-2.52				-4.53			
	15			-3.08		-3.76		-6.67		
	20	-2.53			-2.83		-3.97			

Table 2. Stiffness error results for tensile test

Time (min)		e_D								
		20	18	16	14	12	10	8	6	4
k	2			572.9		166		39.5	26.5	
	3	1952			249.6		82.0		20.5	
	4		439.9			121		31.2		7.0
	5			214.7			54.6		9.6	
	6				110.3	56.7		12.8	13.9	
	8						32.1			
	10	214.5				30.0		9.2	13.6	
	12		122.9				20.4			
	15			99.3		29.7		13.6		
	20	318.1			80.62		23.5			

Table 3. Time results for tensile test

As a first result, it seems that the ratio k does not affect the final stiffness of the strand. The wires are very fine and linear parts and the load is axial. It is important to keep in mind that a tall element damages the global geometry.

In order to compare simultaneously both of the stiffness and the calculation time, we place all the data in a graph to make appear the Pareto Front of the solution (see Figure 5). It shows the optimal values of the problem. Then, we rank the data points before reintroducing them in the design plane (see Figure 6). It creates a map of the optimal solution with in dark green the best solution (great accuracy and low calculation time) and in red the worst ones (either low accuracy or high calculation time).

The optimal values are grouped into 10 or 12 elements in diameter with high length ratio.

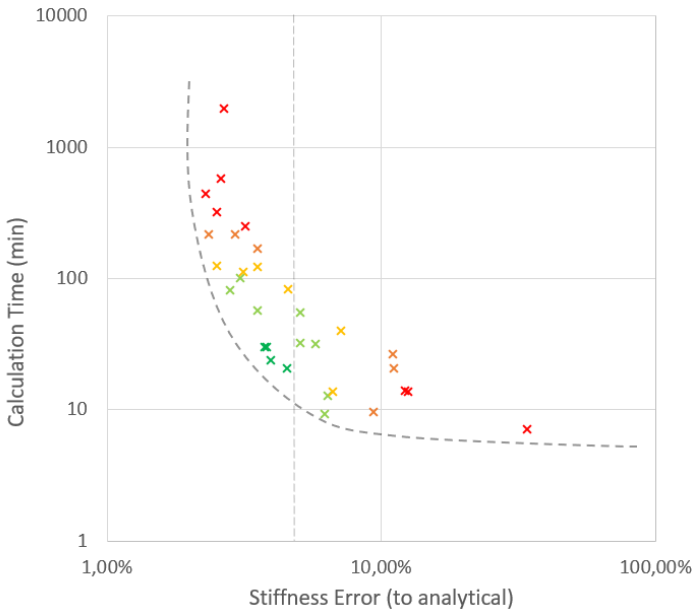

Fig. 5. Tension test Pareto Front

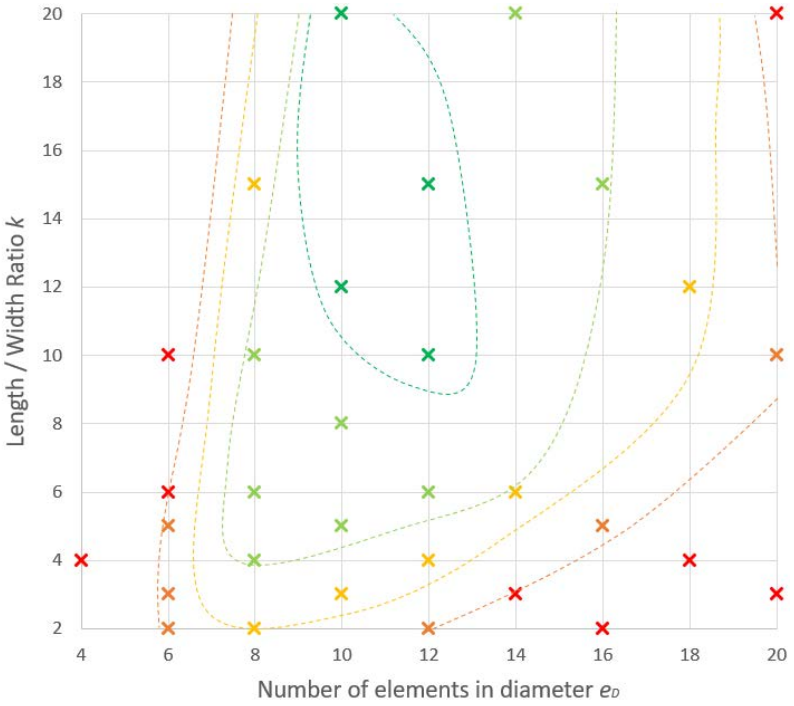

Fig. 6. Tension optimal mesh parameters according to the Pareto Front

4.2 – CRIMPING TEST

In order to clearly highlight the variation of the error with mesh parameters, we exploit a high radial stress value (due to the choice of the crimping depth) with only elastic behavior for the material. For the first time an organized wire strand is modelled for a crimping test.

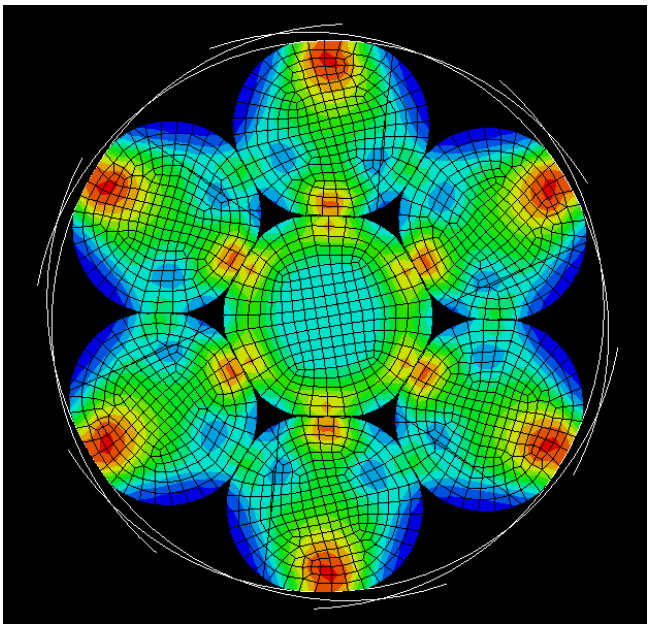

Fig. 7. Stress over the cross section for the crimping test

Figure 7 shows the maximal stress over the cross section is located at the external points of contact of the wires. We can also see the multiple lines of contact within the strand: the three linear lines going through the center and the hexagonal line going through every external wire.

For the crimping test, we use the same sampling process than for tensile test. The reference value is set to be the average maximal stress under the tiles with the higher meshing resolution: "20.3". The label of each curve is written "$e_D.k$". In Fig. 8, we can see the most accurate results for each configuration by number of elements in diameter. First of all, we see a clear peak close to the edge of the tile, at the side where the strand is fixed. This edge effect is due to the brutal stop of the tile and the start of compaction of the strand. It is marked by the choice of the geometry of the tiles (2D and rigid bodies). Then, the undulation of the curves come from the imperfect circular crimping process. When the wires are at the center of a tile, the crimping depth is actual and there is the maximal stress. When the wires are between two tiles, the crimping depth is underestimated and this is the bottom of the waves. This can be avoided by adding more tiles or by choosing another crimping method. Above and equal 16 elements in diameter, the results converge around a single value. The length of the elements does not affect the average of this maximal stress value until this length is greater than the diameter of the wire. It applies only the simultaneous great ratio and low number of elements in diameter.

We apply the same strategy as for tensile test in placing the samples into a calculation time/error graph and draw the associated Pareto front. Then we rank each data (Fig. 9) and replace them in the design plane with our mesh parameters. Thus, we can draw the map of the optimal values for the crimping process (Fig. 10). We obtain the optimal values for high number of elements in diameter (for a greater accuracy) and high ratio k (for a lower calculation time).

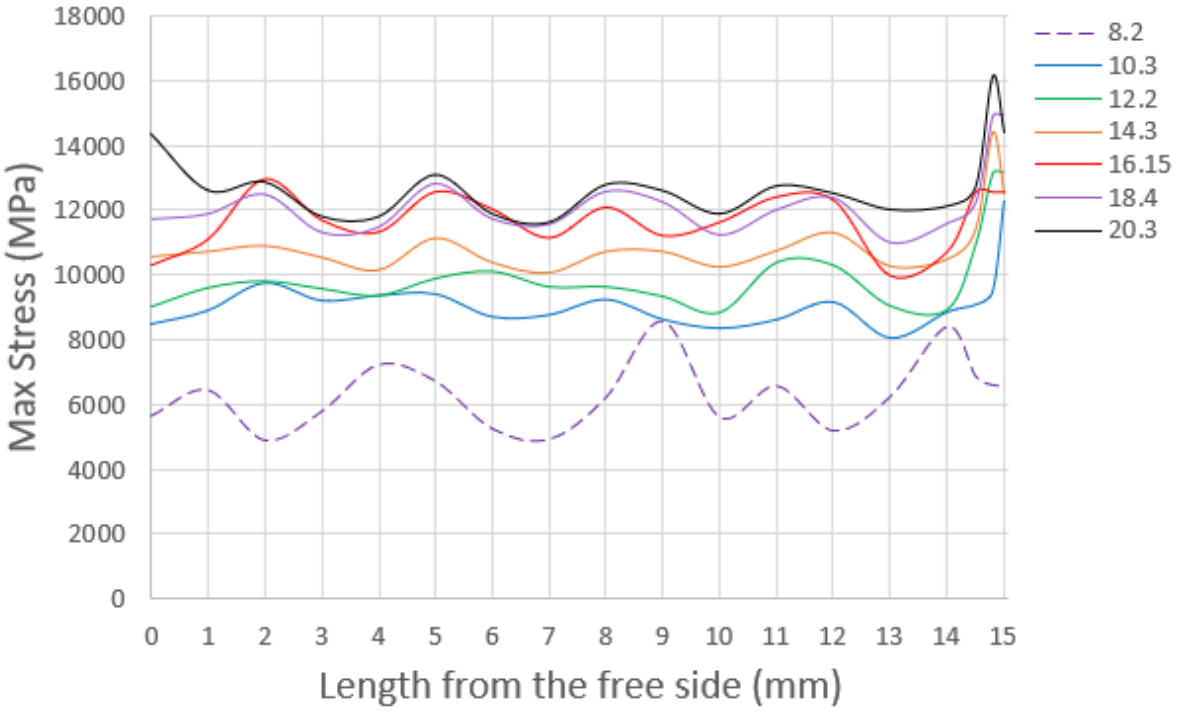

Fig. 8. Maximal stress value for each configuration under the tiles

Time (min)		e_D								
		20	18	16	14	12	10	8	6	4
k	2			769.8		179.0		99.31	Aborted	
	3	1611			280.6		106.4		Aborted	
	4		924.9			104.6		40.4		Aborted
	5			323.5			46.0		Aborted	
	6				105.4	62.4		Aborted	Aborted	
	8						34.7			
	10	198.2				36.1		15.5	Aborted	
	12		153.0				21.4			
	15			64.9		29.3		11.9		
	20	98.1			31.8		13.7			

Table 4. Time results for crimping test

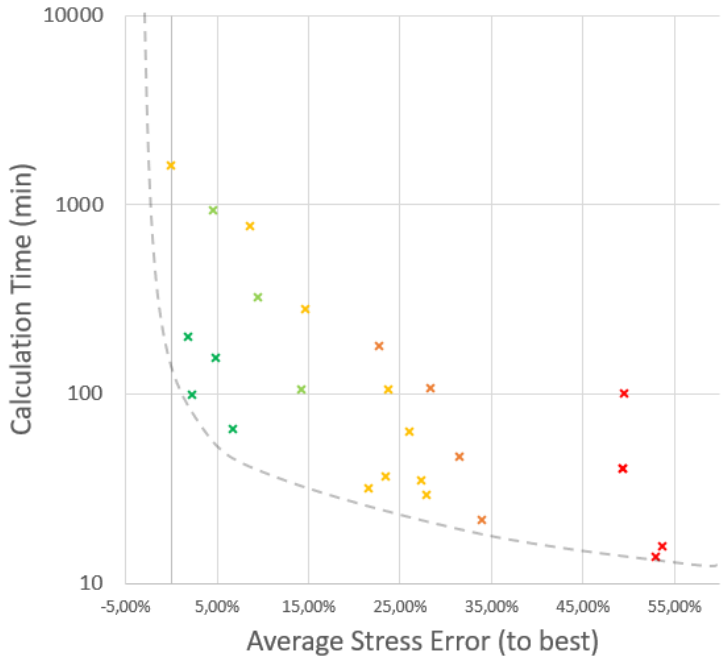

Fig. 9. Crimping test Pareto Front

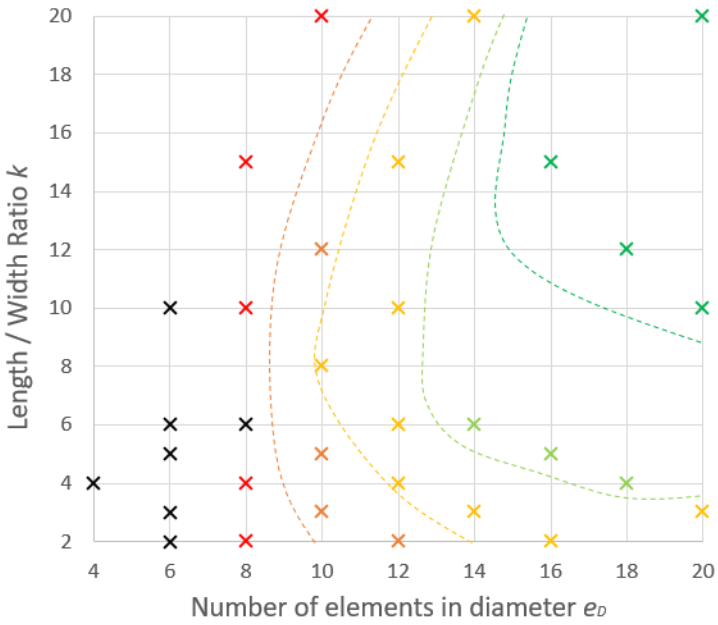

Fig. 10. Crimping optimal mesh parameters according to the Pareto Front

4.3 – COMBINED CIMPING-TENSILE TEST TO MINIMIZE CRIMPING LENGTH

Back to our main issue where the structure is both stressed radially and axially, to plot an optimal solution of combined stressed strand, we superimpose the maps and add up the ranks of each sample. This way, we obtain a new mapping of the stressed wire strand (see Figure 11). The best solution becomes e_D=16 and k=15 as presented in Figure 12. This mesh guarantees both great accuracy with low calculation time.

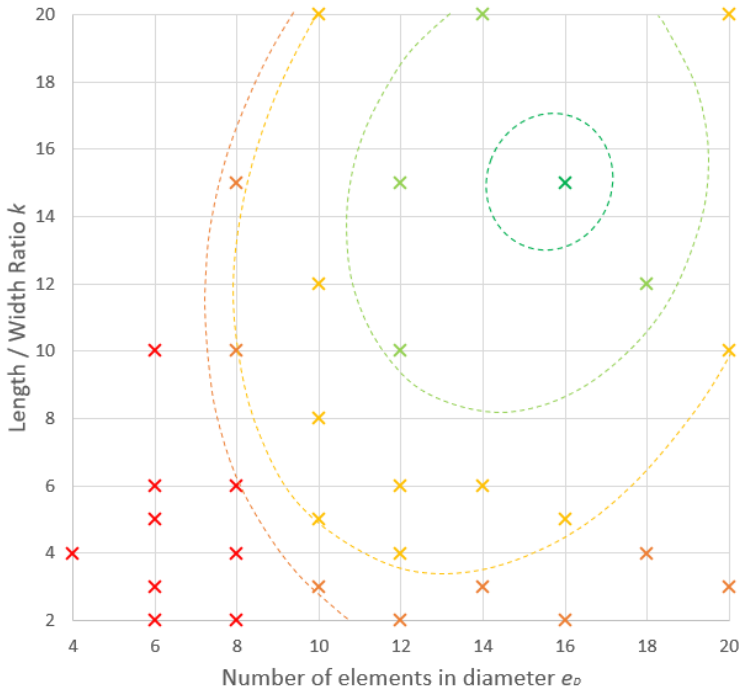

Fig. 11. Combined mapping solution, obtained by superimposing the crimping mapping and the tensile mapping

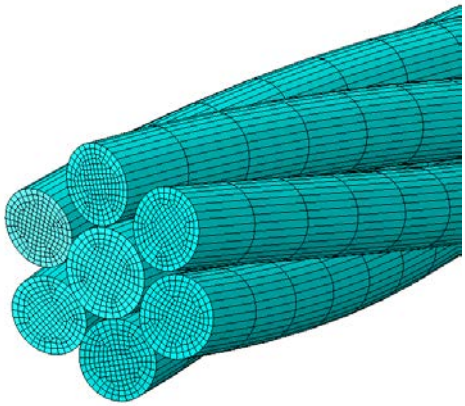

Fig. 12. Optimal mesh solution for combined stress: $e_D = 16$ and $k = 15$

Considering the previous presented work, we are able to construct for the first time a model where the wire rope is stressed radially (crimping test) and axially (tensile test). The model is as follows: a 30mm long single-layered wire strand with the same properties as before, and a cylindrical pipe of internal diameter 1.5mm, thickness 0.05mm and length 20mm (see Figure 13), and the same material as for the wires.

The simulation is done in 4 steps as follows:

1. The internal surface of the pipe is stressed with a uniform pressure to expand the part.
2. Then, the pipe is slid axially until the end of the pipe is 5mm away the end of the rope
3. Pressure is released and the pipe crimps the strand.
4. The external boundary of the pipe is fixed and the tensile load is then set at the free extremity of the rope.

The results shown in Figures 14 and 15 are very promising: the model run in 114 minutes and gives us an acceptable behavior of the strand. The wires do not slip inside the tubular crimp, the axial strain is linear along the free strand, the crimping stress is uniform and reveals a small peak at both its ends. The mesh elements do not over or underestimate the stiffness of the strand in both axial and radial directions.

Fig. 13. Initial position of the model with combined stress using optimal meshing parameters

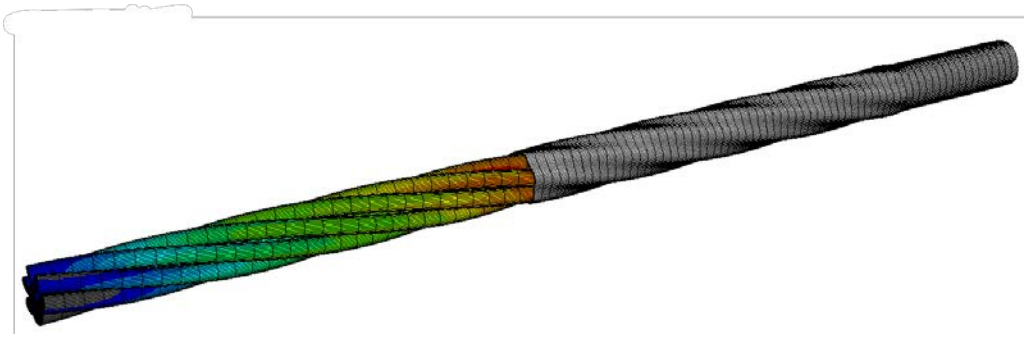

Fig. 14. Axial strain of the final model's wire rope

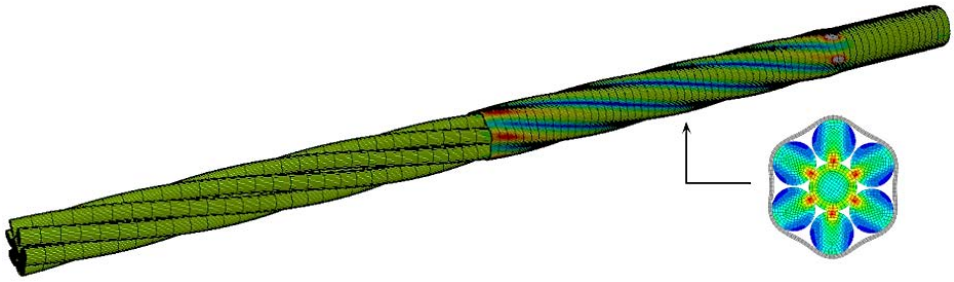

Fig. 15. Stress repartition of the final model with cut view

The final objective is then to optimize the crimping length of the process. To do so, the first simulation used a large crimping length to guarantee the appearance of the two peaks at each side, thus it is possible to identify the non-working area for the axial load transmission and finally remove this area to obtain the optimal crimping length.

We evaluate the axial load transferred from the cable to the pipe and test a potential improvement. In our case, axial load and axial stresses are strongly correlated. Thus, in order to analyze the working crimping zone for tensile test, we evaluate the mean axial stress in the pipe along its crimping length (Figure 16).

For the first time, the analysis of the transmitted axial load between the strand and the crimping part is studied. The variation of axial stress is correlated to the amount of axial load transmitted from the cable to the pipe. Thus, a constant mean axial stress induces that no tensile load is transferred from the cable to the pipe. In this way, the central zone of the crimp is useless. As a consequence, in order to improve the initial design, we decide to 'cut' the pipe from millimeter 4 to 9 in its original crimping length graduation to see if the strength evolves. As a result, with a crimp 5mm shorter, we obtain the same axial stress level as the original crimping (Figure 16). It confirms that the axial load is greatly transmitted at the ends of the crimp and increasing the crimping length more than 10mm (in this case) does not affect the axial strength of the assembly.

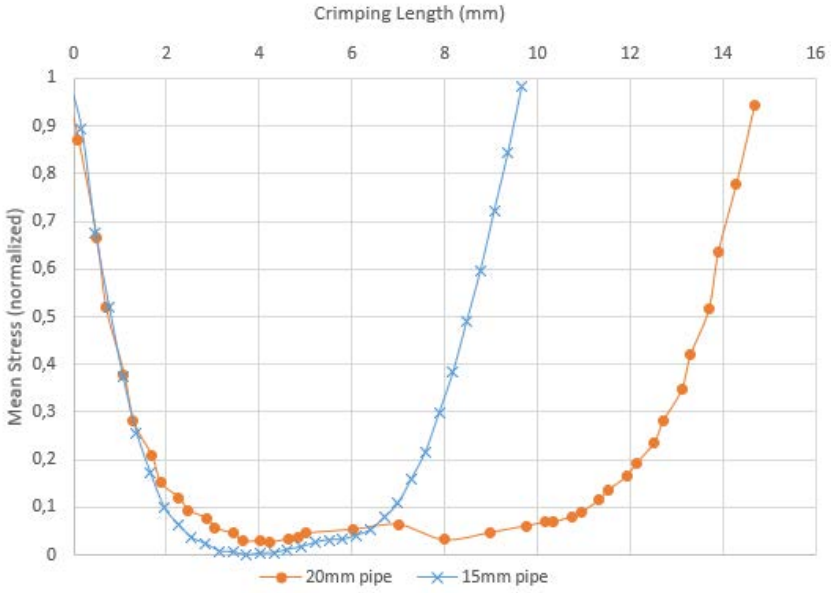

Fig. 16. Mean stress in the pipe cross section along the crimp with in points line the original crimping length stress and in ticks line the optimized crimping length stress

These results can help designers to optimize the crimping length of their process and save lot of production costs. Reducing the crimping length induces both the reduction of the crimp material and the reduction of the necessary crimping load, just like the needed process energy.

5 - CONCLUSIONS

Multi-stranded wire ropes are widely used in engineering applications. In order to reduce cost in 'try and error' time consuming campaigns, numerical simulations became an essential tool for designers. Over the past ten years, finite element simulations have evolved considerably in the field of metal part forming.

In this paper, a numerical model of a single layered wire rope is studied. The objective is to determine the optimal size and shape of meshing elements to get both accurate and fast results. Firstly, the wire strand is investigated in tension. The axial stiffness of the strand is computed and compared with the analytical one formulated by G.A. Costello.

Secondly, the organized wire strand is investigated for the first time in crimping process. The average maximal stress of the strand along the tiles is computed and compared with the numerical test with the highest number of mesh elements.

It has been revealed that the stiffness of a strand does not depend on the mesh length. But this parameter affects the maximal stress during a crimping process. Most of the studies mentioned in the state of the art have in average 6 elements in the diameter and find very divergent results.

The optimal solutions for the studied case 16 elements in the diameter and a length/width ratio=15 for combined stress and very fine mesh length at the crimping border to make visible the edges effect.

This meshing strategy has been efficiently applied to simulate the first ever combined crimping-tensile test and obtain the minimal crimping length successfully. This work was made for a classic lay angle of 80 degrees. For a smaller lay angle, the length of the element must be smaller in order to guarantee a good helical shape. A future study can be led with similar goals under torsion and bending loads.

In conclusion, this work can be very important for designers to reduce considerably the calculation time of their numerical models while guarantying a great accuracy in the behavior and the stiffness of a wire rope. The mesh element size has a significant effect on the global behavior of the strands and must not be neglected. Those preliminary results could be exploited to accurately model more complex wire ropes that can include up to one hundred individual wires.

REFERENCES

[1] P.Zhang, M.Duan, J.Ma, Y.Zhang, A precise mathematical model for geometric modeling of wire rope strands structure, Applied Mathematical Modelling 76, 151-171 (2019). https://www.doi.org/10.1016/j.apm.2019.06.005
[2] G.A.Costello, Mechanics of wire rope, Wire Association International (2003)
[3] C.Erdönmez, N-tuple complex helical geometry modeling using parametric equations, Engineering with Computers, Vol.30, 715- 726 (2014). https://www.doi.org/10.1007/s00366-013-0319-9
[4] A.E.H.Love, A treatise on the mathematical theory of elasticity, Vol.1, 1st edition (1892)
[5] S.Timoshenko, Strength of Materials, Parts I and II, 1st edition (1930)
[6] F.H.Hruska, Calculation of stresses in wire ropes, Wire Prod Vol.26 (9), 766–767 (1955)
[7] A.E.Green, N.Laws, A general theory of rods, Springer, 1st edition (1966)
[8] E.Kroner, Mechanics of generalized continua, Springer, 1st edition (1967)
[9] G.A.Costello, Theory of wire rope, 2nd edition Springer, 14-28 (1997)
[10] W. Zhou, H.Q.Tian, A novel finite element model for single-layered wire strand, Journal of Central South University Springer, 20, 1767-1771 (2013). https://www.doi.org/10.1007/s11771-013-1670-0
[11] S. Wang, Z. Wang, J. Gong, Y. Wang and Q. Huang. Coupling effect analysis of tension and reverse torque during axial tensile test of anchor cable. Dyna. May 95. (2020):288-293. https://dx.doi.org/10.6036/9603
[12] F.M.Filotto, F.Runkel, G.Kress, Cross section shape optimization of wirestrands subjected to purely tensile loads using a reduced helical model, Advanced modeling and simulation in Engineering science, 7 :23 (2020). https://www.doi.org/10.1186/s40323-020-00159-0
[13] W.G.Jiang, J.L.Henshall, J.M.Walton, A concise finite element model for three-layered straight wire rope strand, International Journal of Mechanical Sciences, 42, 63-86 (2000) https://doi.org/10.1016/S0020-7403(98)00111-8
[14] J.M.Atienza, J.Ruiz-Hervias, L.Caballero, M.Elices, Role of temperature and stretching force on the effictiveness of the stabilizing treatment of prestressing steel wires, Conference Proceedings for the 81st annual convention of the Wire Association International (2011)
[15] I.Gerdemeli, S.Kurt, A.S.Anil, Analysis with finite element method of wire rope, Machines, Technologies, Materials, Vol.2, 107-110 (2012)
[16] Wolfram Demonstration project, Dimensions of a Stranded Wire, https://demonstrations.wolfram.com/DimensionsOfAStrandedWire/ [accessed 03 May 2022]
[17] C.Erdonmez, C.E.Imrak, Modeling And Numerical Analysis Of The Wire Strand, Journal of Naval science and Engineering, Vol.5, 30-38 (2009)
[18] R.C.Wang, A.J.Miscoe, W.M.McKewan, Model for the structure of round-strand wire ropes, Report of investigation 9644, NIOSH (1998)
[19] C.Erdönmez, A general scheme to create complex triple helical wire rope model using parametric equations, Journal of Science and Engineering, 20 (2018). https://www.doi.org/10.21205/deufmd.2018206071
[20] C.E.Imrak, C.Erdönmez, On the problem of wire rope model generation with axial loading, Mathematical and Computing Applications, Vol.5, No.2, 259-268 (2010). https://www.doi.org/10.3390/mca15020259
[21] R.K.Kumar, A.S.Babu, Evaluation of mechanical crimping process using finite element analysis, First International Conference on Structural Integrity (2014)
[22] R.K.Kumar, A.S.Babu, Finite element analysis and experimental study on metal joining by mechanical crimping, International Journal of Service and Computing Oriented Manufacturing, Vol.1, No.4 (2014). https://www.doi.org/10.1504/IJSCOM.2014.066489
[23] W.Yang, S.Wang, Y.Zhao, S.Wang, C.Ma, X.Li, Z.Liu, Deformation-based accurate geometric model of stranded wire helical spring, International Journal of Mechanics and Materials in Design, Vol(16), 589-617 (2020). https://www.doi.org/10.1007/s10999-020-09490-1
[24] A.Schiavone, T.Y.Qiu, L.G.Zhao, Crimping and deployment of metallic and polymeric stents -- finite element modelling, Vessel Plus, 12-21 (2017). https://www.doi.org/10.20517/2574-1209.2016.03
[25] Abaqus Documentation V6.6: Element Librairy Overview, https://classes.engineering.wustl.edu/2009/spring/mase5513/abaqus/docs/v6.6/books/usb/default.htm?startat=pt06ch23s06alm15.html [accessed 03 May 2022]
[26] D.V.Zhmurkin, N.E.Corman, C.D.Copper, R.D.Hilty, 3-Dimensional Numerical Simulation of open-barrel crimping process, Institute of Electrics and Electronics Engineers (2008). https://www.doi.org/10.1109/HOLM.2008.ECP.41
[27] S.M.Gu, H.S.Choi, Y.S.Kim, Effects of Design Variables on compression rate of wire in connector crimping process of wire harness using FEM, Transactions of Materials Processing, Vol.19, No.5 (2010). https://www.doi.org/10.5228/KSPP.2010.19.5.305
[28] X.Cao, W.Wu, The establishment of a mechanics model of multi-strand wire rope subjected to bending load with finite element simulation and experimental verification, International Journal of Mechanical Sciences, 289-303 (2018). https://doi.org/10.1016/j.ijmecsci.2018.04.051
[29] C.Erdonmez, Analysis and design of compacted IWRC meshed model under axial strain, International Journal of Mechanics and Materials in Design, Vol(16), 647-661 (2020). https://doi.org/10.1007/s10999-019-09481-x
[30] C.Lange, Etude physique et modélisation numérique du procédé de sertissage de pièces de carrosserie, PhD thesis, Ecole nationale supérieure des mines de Paris (2006)
[31] W.G.Jiang, A concise finite element model for pure bending analysis of simple wire strand, International Journal of Mechanical Sciences, 54, 69-73 (2012). https://doi.org/10.1016/j.ijmecsci.2011.09.008
[32] H.Li, T.Yamada, P.Jolivet,K.Furuta, T.Kondoh, K.Izui, S.Nishiwaki, Full-scale 3D structural topology optimization using adaptive mesh refinement based on the level-set method, Finite Elements in Analysis and Design, Vol(194) (2021). https://doi.org/10.1016/j.finel.2021.103561
[33] A.Lamecki, A.Dziekonski, Lukasz Balewski, G.Fotyga, M.Mrozowski, GPU-Accelerated 3D mesh deformation for optimization based on the finite element method, Radioengineering, Vol(26), 924-929 (2017). https://doi.org/10.13164/re.2017.0924
[34] S.R.Ghoreishi, T.Messager, P.Cartraud, P.Davies, Validity and limitations of linear analytical models for steel wire strands under axial loading, using a 3D FE model, International Journal of Mechanical Sciences, 49, 1251-1261 (2007). https://doi.org/10.1016/j.ijmecsci.2007.03.014